Population connectivity predicts vulnerability to white-nose syndrome in the Chilean myotis (*Myotis chiloensis*) - a genomics approach

Thomas M. Lilley, *[1] Tiina M. Sävilammi TM, † Gonzalo Ossa, ‡§ Anna S Blomberg, † Anti Vasemägi, ** Veronica Yung, †† David L.J. Vendrami, ‡‡ Joseph S Johnson §§

* Finnish Museum of Natural History, University of Helsinki, Helsinki, Finland.
† Department of Biology, University of Turku, Turku, Finland.
‡ ConserBat EIRL, San Fabian, Chile
§ Programa para la Conservación de los Murciélagos de Chile, Santiago, Chile
** Department of Aquatic Resources, Swedish University of Agricultural Sciences, Uppsala, Sweden
†† Sección Rabia, Subdepartamento de Enfermedades Virales, Instituto de Salud Pública, Santiago, Chile
‡‡ Department of Animal Behavior, University of Bielefeld, Bielefeld, Germany
§§ Department of Biological Sciences, Ohio University, Athens, Ohio

Corresponding author: Thomas M. Lilley

ORCiD:

Thomas M. Lilley: 0000-0001-5864-4958

Tiina M. Sävilammi: 0000-0001-9836-3843

Anna S. Blomberg: 0000-0002-6754-4948

David L.J. Vendrami: 0000-0001-9409-4084

Joseph S. Johnson: 0000-0003-2555-8142

Data availability

The RAD sequencing reads were deposited at NCBI SRA under BioProject ID PRJNA596389.

Running title: Population structure of *Myotis chiloensis*

Key words: Population genetics, population connectivity, population structure, chiroptera, disease spread.

[1] Finnish Museum of Natural History, P. Rautatiekatu 13, University of Helsinki, PL 17, 00014 Helsinki, Finland

Phone: +358408337783

Email: thomas.lilley@helsinki.fi

ABSTRACT

Despite its peculiar distribution, the biology of the southernmost bat species in the world, the Chilean myotis (*Myotis chiloensis*), has garnered little attention so far. The species has a north-south distribution of c. 2800 km, mostly on the eastern side of the Andes mountain range. Use of extended torpor occurs in the southernmost portion of the range, putting the species at risk of bat white-nose syndrome (WNS), a fungal disease responsible for massive population declines in North American bats. Here, we examined how geographic distance and topology would be reflected in the population structure of *M. chiloensis* along the majority of its range using a double digestion RAD-tag method. We sampled 66 individuals across the species range and discovered pronounced isolation-by-distance. Furthermore, and surprisingly, we found higher degrees of heterozygosity in the southernmost populations compared to the north. A coalescence analysis revealed that our populations may still not have reached secondary contact after the Last Glacial Maximum. As for the potential spread of pathogens, such as the fungus causing WNS, connectivity among populations was noticeably low, especially between the southern hibernatory populations in the Magallanes and Tierra del Fuego, and more northerly populations. This suggests the probability of geographic spread of the disease from the north through bat-to-bat contact to susceptible populations is low. The study presents a rare case of defined population structure in a bat species and warrants further research on the underlying factors contributing to this.

Key words: population structure, Myotis, Chiroptera, opportunistic pathogen, disease spread

63 INTRODUCTION

64 Transmission of infectious diseases has garnered attention as one of the greatest risks to
65 human, agriculture and wildlife health over the last decade (Cangelosi *et al.* 2004; Semenza
66 and Menne 2009). Previous research demonstrates that the emergence of previously
67 unknown diseases often results from a change in the ecology of the host, pathogen, and/or
68 their environment (Scholthof 2007). An example of this is white-nose syndrome (hereafter
69 WNS), an epizootic disease that emerged in North America in 2006 (Blehert *et al.* 2009). The
70 disease is caused by the fungus, *Pseudogymnoascus destructans*, which infects insectivorous
71 bats during the hibernation period at latitudes where prey are not widely available during
72 winter (Lorch *et al.* 2011). Populations of highly susceptible species, especially from the
73 genus *Myotis*, have declined by >90% in areas affected by WNS (Frick *et al.* 2010). The
74 opportunistic pathogen can utilize alternative carbon sources (Raudabaugh and Miller 2013)
75 and can persist in the cold, humid environment within hibernacula in the absence of bat
76 hosts (Lorch *et al.* 2013; Hoyt *et al.* 2014).

77 *P. destructans* is native to Eurasia, where it has a large geographic range, with transmission
78 to North America likely facilitated by humans (Warnecke *et al.* 2012; Leopardi *et al.* 2015).
79 In North America, bats suffering from WNS were first detected in the state of New York
80 during the winter of 2006–2007 (Frick *et al.* 2010). The fungus has since spread across North
81 America, with records of prevalence in 33 U.S. states and 7 Canadian provinces. So far, *P.*
82 *destructans* has been detected on 17 species of bats, with more species likely to follow.
83 While human-assisted transmission of *P. destructans* likely has contributed to this spread,
84 the ecology and behaviour of cave-hibernating bats in North America also makes them
85 efficient vectors over large geographic areas (Wilder *et al.* 2015). Because WNS affects bats
86 during extended bouts of torpor, at low temperatures where it is able to grow and infect the
87 host, there has been speculation over how far into the southern North America the disease
88 will spread (Verant *et al.* 2012; Meierhofer *et al.* 2019). Although bats inhabiting lower
89 latitudes may suffer less from WNS, *P. destructans* conidia may be able to survive on the
90 body of bats for several months, even at temperatures up to 37 °C (Campbell *et al.* 2019).
91 This could facilitate the movement of WNS across Mesoamerica and the tropics, to arrive to

high southern latitudes where bats may be susceptible (Holz *et al.* 2019; Turbill and Welbergen 2019).

Of species known to harbour the WNS fungus, *Tadarida brasiliensis* is of particular interest. As a long-range migratory species, with movements spanning thousands of kilometres (Cockrum 1969; Glass 1982), *T. brasiliensis* may be an important vector for spreading *P. destructans* into the southern hemisphere (Ommundsen *et al.* 2017; McCracken *et al.* 2018). Ecological niche models predict suitable habitat for the proliferation of *P. destructans* in South America, highlighting the need to understand vectors such as *T. brasiliensis* as well as human transmission (Escobar *et al.* 2014). However, once *P. destructans* arrives in South America, its spread will not necessarily resemble that seen in North America, as it is likely to be influenced by differing geology and species ecology.

The Chilean myotis (*Myotis chiloensis* [Waterhouse, 1840]) is the most Southerly distributed species of bat in the world, together with the southern big-eared brown bat (*Histiotus magellanicus*, Koopman 1967; Gardner 2007). *Myotis chiloensis* has a vast north-south distribution that includes forested areas on both sides of the Andes from the northern shore of Navarino Island to the southern border of the Atacama desert in Chile (Ossa and Rodriguez-San Pedro 2015). The range of *M. chiloensis* overlaps with the distribution of *T. brasiliensis* from the north, where *M. chiloensis* is not believed to hibernate, to 45°S latitude, where *M. chiloensis* possibly hibernate and may therefore be susceptible to WNS (Bozinovic *et al.* 1985). However, there is no information available on the population structure of *M. chiloensis*, precluding an understanding of how *P. destructans* could be transported from the northern edge of its range to more southern, and vulnerable, populations. The connectedness of individuals across the range will determine the speed and intensity of potential spread. Population structuring in bats is often relatively low because of their efficient mode of dispersal, flight (Laine *et al.* 2013). An ability to disperse more efficiently results in decreased population differentiation (Bohonak 1999) to the extent that some bat species are panmictic across their range (Burland and Wilmer 2001; Laine *et al.* 2013). Such high dispersal would likely result in rapid spread of *P. destructans*. However, bats in the genus *Myotis* show instances of pronounced population structure that may hinder spread of the fungus. For instance, the Gibraltar Strait, which separates the

122 Iberian Peninsula from the Maghreb in Morocco by a minimum gap of 14 km of the open
123 sea, represents a barrier for gene flow for *M. myotis* (Castella *et al.* 2000). Chile is littered
124 with such potential barriers to gene flow, such as the Atacama Desert, glaciers, ice fields,
125 the Andes Mountains, and the Magellan Strait, which in turn can hinder the potential spread
126 of *P. destructans*. Furthermore, populations may still be affected by the Last Glacial
127 Maximum, which covered a large part of Patagonia under ice until c. 10000 years bp (Sérsic
128 *et al.* 2011; Mansilla *et al.* 2018).

129 With tourism in southern Chile expected to increase (e.g. . http://www.conaf.cl/parques-
130 nacionales/visitanos/estadisticas-de-visitacion/), and migratory species such as *T.*
131 *brasiliensis* capable of carrying spores across large distances, there is a serious need to
132 better understand the population structure of Patagonian bat species before WNS spreads
133 to the region. The lack of knowledge on the extent of migration and mixing, and life history
134 traits in general, means that research in this area is now urgent and essential (Ossa and
135 Rodriguez-San Pedro 2015; Ossa 2016; Ossa *et al.* 2019). Studying population ecology
136 through molecular genetic methods allows for the identification of more accurate
137 population boundaries, which is important when assessing conservation in response to
138 threats of disease and dramatic declines in population size (Moritz 1994). This study will
139 therefore aim to describe population structure and isolation-by-distance in *M. chiloensis*
140 across the range of the species. By studying *M. chiloensis* along 2400 km of latitudinal
141 gradient using genome-wide SNP markers, we aimed to test if geography and the Last
142 Glacial Maximum influence genetic isolation patterns.

143 MATERIALS AND METHODS

144 Sample collection and DNA extraction

145 To describe population genetic structure in *M. chiloensis*, we obtained wing tissue samples
146 of 66 bats from two sources. A portion were obtained from live bats captured in the field
147 during November and December 2017 (i.e. austral spring) from two localities: Chicauma,
148 Metropolitana region (33 °S 70 °W) and Karukinka Reserve, Tierra del Fuego (64 °S 78 °W)
149 respectively (Capture permit: 4924_2017, Figure 1 A, Table S1). We used disposable biopsy
150 punches (5 mmm, MLT3335, Miltex Instrument Co, Plainsboro, New Jersey) to collect tissue

151 samples from the plagiopatagium of captured, live bats. The sampled bats were released at
152 the capture site. Additional samples were obtained from dead bats submitted to the Public
153 Health Institute of Chile for rabies testing (Figure 1 A, Table S1). Submitted bats included
154 latitude and longitude locations of origin. Tissue samples from the bats submitted for rabies
155 testing were obtained from the plagiopatium using sterile scalpels. To determine if *P.*
156 *destructans* had already spread to Chile, we swabbed the nose and wings of all bats in the
157 field and at the Public Health Institute of Chile bat with a sterile polyester swab (Puritan 25-
158 806 1PD, Guildford ME, USA) and stored at -20 °C until analysis.

159 We divided samples into four groups according to their geographic origin, with sub-locations
160 within each group to assist in further analyses. Sampling locations are presented in Figure 1
161 A and details of populations and samples are provided in Table 1 and Table S1. Tissue
162 samples were stored in 1.5 ml tubes with 95% EtOH and stored at -20 °C until further
163 analysis. Fungal spore samples were stored in 1.5 ml tubes and stored at -20 °C until further
164 analysis. We extracted DNA from tissue samples using QIAmp DNA Mini Kits (Qiagen, Hilden
165 Germany) and stored DNA at -80 °C. DNA from fungal swabs was extracted using Qlamp
166 DNA Micro Kits (Qiagen, Hilden Germany).

167 The amount of DNA in the final solution of each sample was tested and quantified using the
168 Thermo Scientific Nanodrop spectrophotometer, giving a result for the amount of DNA in
169 ng/ µL. Samples were frozen between DNA extraction and analysis.

170 Identification and quantification of *P. destructans*

171 Quantification of *P.destructans* load by qPCR was completed as described previously in
172 Johnson et al. (2015) with the exception of using 1 µl sample in the reaction, Roche Fast
173 Start Essential DNA Probe Master, and a Roche Lightcycler 480 instead of a BioRad iCycler.

174 RAD sequencing

175 We sequenced 66 individuals in total. Duplicate samples from 30 individuals were
176 additionally sequenced to estimate repeatability and error rate of the called genotypes.
177 DNA was prepared for genotyping-by-sequencing using a double digestion RAD-tag method
178 as described in Elshire et al. (2011). PstI-BamHI-digested libraries were prepared by the

179 Center of Evolutionary Applications (University of Turku; see Lemopoulos et al. 2017 and
180 references therein for further details) and sequenced in an Illumina HiSeq2500 run (100 bp
181 single end reads and pooling 96 samples on each lane) at Finnish Functional Genomics
182 Centre (Turku Bioscience).

183 Yield comparison samples

184 As the amount of DNA available may often be very limited in experiments where preserved
185 samples from the rabies laboratory are utilized, we wanted to estimate the effect of initial
186 DNA concentration to the resulting read coverage. We compared the total read coverages
187 of the replicate samples with Pearson's correlation.

188 The resulting fastq reads, separated by barcode for each sample, were quality-controlled
189 and low-quality bases trimmed with condetri v. 2.3 with parameter minlen=30 (min. length
190 of a trimmed read) followed by adapter-trim with cutadapt for Illumina universal adapters
191 from the end of the reads (identified with FastQC quality control in some of the samples).
192 Then, reads were mapped against *M. lucifugus* genome (mluc_2.0_assembly_supers.fasta)
193 using bwa mem with parameters -B 3 -O 5 -k 15. After mapping back with BWA mem, we
194 used SAMtools v. 1.4 and the associated bcftools for calling genotypes for SNPs and for
195 filtering SNPs based on minimum of 40% of the samples genotyped, at least eight
196 alternative alleles detected and SNP quality >=20 (bcftools filter). We further filtered the
197 SNPs based on exactly two alleles detected and excluded SNPs with particularly low (≤5) or
198 unusually high (≥125) mean coverage based on visual inspection of the mean coverage
199 distribution.

200 Population genetic analysis

201 For the final SNP dataset, which only included unduplicated samples, we performed
202 principal component analysis implemented in prcomp function of R stats package, and
203 calculated Euclidean genetic coordinates for each individual from PC1 and PC2. The four
204 pre-determined ancestral populations based on the sampling regions of each individual
205 were confirmed by hierarchical clustering of the Euclidean distanced calculated from PC1
206 and PC2. Individuals clustering to a neighbouring population were assumed to have
207 dispersed from their natal populations and were reassigned for the later analysis. We

208 further investigated the relative contributions of the ancestral populations inhabiting
209 regions 1-4 in the present-day nucleotide using ADMIXTURE (Zhou et al. 2009) analysis for
210 the A-samples, run with four expected populations (parameter K=4) based on prior
211 knowledge of the population structure, and with quasi-Newton convergence acceleration
212 method. We were particularly interested in identifying possible hybrid individuals.

213 After assigning each individual to the final regions, we calculated Nei's pairwise F_{ST} using
214 HierFSTat v. 0.04-22 pairwise. FST function for A-samples for SNP's with no missing values.
215 To assess the significance of genetic differentiation, we compared the actual obtained F_{ST}
216 estimates to the null distributions of F_{ST} values under panmixia, obtained from a hundred
217 random permutations of alleles. Latitude and longitude coordinates of the sampling
218 locations were used to calculate pairwise geographic distances between individuals in
219 kilometres using Haversine method assuming a spherical earth, implemented in function
220 distm in the R package geodist v. 1.5-10.

221 We estimated Isolation-by-distance with two methods: A Mantel test with complete
222 permutations and a linear model *geographic distance ~ genetic distance*. We used pairwise
223 F_{ST} as a measure for the genetic distances and mean of between-individual distances as
224 geographic coordinates for populations inhabiting each of the four regions. To study the
225 population structure in more detail, we repeated the Isolation-by-distance analysis for the
226 genetic vs. geographic distances from the most extreme individual (sample ID 700) using a
227 Mantel test with all possible permutations, and a linear model to identify individuals with
228 unusually high or low genetic differentiation. We then studied the systematic differentiation
229 of the individuals sampled in different regions by assessing the differences of the residual
230 distributions of each of the four populations from zero using t-tests and Bonferroni-
231 correction of the *P*-values.

232 We also calculated mean observed heterozygosity within the variable loci in Hardy-
233 Weinberg equilibrium (*FDR*>=0.05) in each of the four study regions and compared the
234 observed values to the mean expected heterozygosities using inbreeding coefficient *F,*
235 calculated as the difference between expected and observed heterozygosity divided by
236 expected heterozygosity (Serre 2006). The 95% confidence intervals for the heterozygosity
237 estimates were found by randomly sampling the variable loci for 1,000 times and extracting

238 the distributions of bootstrap means. The deviations of *F* statistics from zero were detected
239 using single-sample Wilcoxon tests. The significances of the regional differences in the
240 observed and expected heterozygosity distributions, and in the F statistics, were tested both
241 by inspecting the overlaps in the bootstrapped confidence intervals and using analysis of
242 variance and Tukey's post hoc tests. The significances of within-region differences between
243 the expected and observed heterozygosity were tested both by comparing the
244 bootstrapped confidence intervals and by pairwise t-tests and Bonferroni-corrected p-
245 values. Finally, the fraction of SNPs unique to any one region, and the number of SNPs
246 shared between all regions, were calculated from the observations of variable and non-
247 variable loci within regions.

248 Demographic modeling

249 To formally test whether any of the studied populations experienced secondary contact
250 following glaciation, we implemented a demographic analysis using the software
251 *fastsimcoal2* (Excoffier *et al.* 2013) in combination with the folded site frequency spectra
252 (SFS) calculated from our data using easySFS.py utility (available from
253 https://github.com/isaacovercast/easySFS). Specifically, we evaluated support for two
254 alternative models (Supplementary Figure S6). The first model, representing our null
255 hypothesis of no secondary contact among populations, specified four distinct lineages
256 (region 1, region 2, region 3 and region 4) corresponding to the populations inhabiting the
257 four geographic regions sampled in the present study. These diverged from each other at
258 the time points T1, T2 and T3 as presented in Figure S6a, and exchanged no migrants.
259 Region 1 was used as the lineage from which the other three populations emerged, as this is
260 thought to be the population which is closest to the ancestral *Myotis chiloensis* population.
261 The second model, representing our alternative hypothesis of secondary contact among
262 populations, was identical with the exception that symmetric migration was present
263 between population pairs region 1- region 2 and region 3- region 4, and asymmetric
264 migration was implemented from region 2 to region 3 (Supplementary Figure S6b). In
265 addition to identify the model that was best supported by our data, we also estimated
266 divergence times (T1, T2 and T3) and effective population sizes (region 1, region 2, region 3

267 and region 4) for the four modeled lineages, as well as migration rates (Mig12, Mig21,
268 Mig34, Mig43 and Mig32).

269 We performed 50 independent *fastsimcoal2* runs for each model, with 100,000 simulations
270 and 40 cycles of the likelihood maximization algorithm. We then calculated Akaike's
271 Information Criteria (AIC) from the *fastsimcoal2* runs which yielded the highest maximum
272 likelihood for each model and used these values for model comparison. Finally, we
273 extracted parameter estimates from the best run of the most supported model and
274 calculated 95% confidence intervals based on 100 parametric bootstrap replicates, as
275 described in Excoffier et al. (2013).

276 Data availability

277 The RAD sequencing reads were deposited at NCBI SRA under BioProject ID PRJNA596389.

278 RESULTS

279 Filtering

280 Ninety-one of the 96 samples (66 individuals and 30 duplicates) had reads matched with a
281 barcode. Of the obtained genotypes, 54846 were biallelic and used in the later analysis,
282 while we excluded 88882 non-variable (homozygous to alternative) variants and 1708
283 variants with more than 2 alleles. After filtering, the mean SNP coverage ranged from 0.5 to
284 257.0 (Supplementary Figure S1). We excluded tags with < 5 or > 125 mean coverage,
285 leaving 47079 tags. The average rate of missing SNPs among the final unique samples was
286 6.2%, ranging from 0 to 24%.

287 Replicate samples

288 The correlation between input DNA concentration and the resulting mean per-sample read
289 coverage was only moderate (cor = 0.3394, t_{61} = 2.8178, P = 0.0065, Supplementary Figure
290 S2 A, Supplementary Figure 3 A-B). In contrast, we found strong and negative association
291 between mean read coverage after sequence assembly and the number of missing genotype
292 calls (cor = -0.9763, t_{61} = -35.223, P < 2.2e-16, Figure S2 B). Furthermore, read coverages
293 were very similar between the technical replicate samples (cor = 0.8736, t_{26} = 9.1542, P =

294 1.292e-09, Supplementary figure S2 C), allowing us to omit "B" samples (replicated). The
295 removal of the biological replicates was conducted to minimise the possible SNP calling bias
296 induced by some samples having approximately twice the amount of sequence data
297 compared to the others, if replicate samples had been combined. Identical genotype calls
298 ranged from 85.6% to 96.9% with an average of 94.2% identical genotype calls
299 (Supplementary figure S3 C), depending heavily on read coverage (cor = 0.9275, t_{26} = 12.641,
300 *P* = 1.312e-12 and cor = 0.8484, t_{26} = 8.1716, *P* = 1.186e-08 in "A" and "B" samples,
301 respectively; Supplementary figure 2 E-F). Although the correlation between the initial DNA
302 concentration and identical genotype calls between biological replicates was significant (cor
303 = 0.5990, t_{26} = 3.814, *P* = 0.0007579; Supplementary figure S2 D), this seemed to mainly be
304 due to two outlier observations with both very low concentration and repeatability.

305 Identification and quantification of *P. destructans*

306 Besides our control samples, no samples showed signs of amplification a portion of the
307 multicopy intergenic spacer region of the rRNA gene complex of *P. destructans* by 38 cycles,
308 which is generally considered as a cut-off for the presence of the pathogen DNA in the
309 samples (Muller *et al.* 2013). Therefore, we can conclude that the *M. chiloensis* individuals
310 sampled in this study did not carry *P. destructans*.

311 Population genetic analysis

312 Principal component analysis on 66 individuals and 5538 SNPs without any missing values
313 from non-duplicated samples (label including A, Figure 1 B) revealed a clear structuring of
314 individuals according to the sampling location indicative of strong population structure.
315 Based on hierarchical clustering of the two most important principal components
316 (Supplementary Figure 4), we confirmed the four pre-determined populations based on the
317 natural hierarchical structuring of the data. Based on the clustering, the sub-population
318 assignment of one individual, sample number 679, changed from Biobio to Maule (which
319 was the most common region assignment among the three nearest neighbors for that
320 individual). The estimation of ancestry of each sampled individual by examining the relative
321 contributions of ancestral populations inhabiting regions 1-4 in the present-day revealed

322 particularly pure ancestral lines in the northern and southern parts of the range, with
323 hybridization occurring in the central part of the range (Figure 2.).

324 Pairwise F_{ST}-value estimates between the populations sampled from the four geographical
325 locations ranged from 0.04 (between regions 2 and 3) to 0.113 (between the most distant
326 regions 1 and 4, Table 2). All estimated F_{ST} values were found significantly larger (P<0.01)
327 than the permuted F_{ST} distributions, with the 95 % confidence intervals of the null
328 distributions between 0 and 0.0205. Both the Mantel test approach and linear modelling
329 between genetic distances (Euclidean distances calculated from PC1 and PC2) and
330 geographical distances (latitude/longitude coordinates converted to distances in kilometres)
331 strongly suggested that we reject the null hypothesis of geographic and genetic distances
332 being unrelated. For the between-population comparisons with F_{ST}, we calculated Mantel
333 statistic r = 0.9497 (P = 0.041667) and R-squared estimate of 0.8773 (DF = 1,4, t = 6.063, P =
334 0.00374) (Supplementary figure 5. Also, for the between-individual distances, the observed
335 Mantel statistic r = 0.944 (P = 0.001), and R-squared estimate 0.943 (DF = 1,61; t = 31.994; P
336 < 2e-16) from the linear modelling suggesting that genetic and geographic distances are
337 strongly positively associated (Figure 3). More detailed exploration of the between-
338 individual linear model revealed, that the distribution of the residuals in regions 1 (DF = 20, t
339 = -3.0679, Bonferroni P = 0.024284) and 4 (DF = 11, t = -10.523, Bonferroni P = 1.7724e-06)
340 were marginally smaller than 0, while the residuals of individuals in regions 2 (DF = 15; t =
341 3.5896; adj. Bonferroni P = 0.002682) and 3 (DF = 13, t = 5.9325, Bonferroni P = 0.0001986)
342 were significantly larger than 0 (Figure 3).

343 Of the total of 47079 SNPs, 43903 were found to be in Hardy-Weinberg equilibrium.
344 Analyses of variance revealed statistically significant differences between populations in
345 observed heterozygosities [F(3,106450)=760.6, P<2e-16], in expected heterozygosities
346 [F(3,106450)=871.4, P<2e-16], and in the F statistics [F(3,106450)=55.29, P<2e-16]. Both
347 based on confidence intervals and pairwise comparisons, observed and expected
348 heterozygosity distributions were consistently higher (non-overlapping 95% confidence
349 intervals and adjusted P<0.05) in the southern regions than in north, except for the two
350 northernmost regions (region 1 vs. region 2), where a statistically significant difference was
351 not observed (Table 1, Table S2). Similarly, observed heterozygosities were consistently

352 lower than those estimated from allele frequencies (non-overlapping 95% confidence
353 intervals and adjusted $P<0.05$), which may be caused by within-region population structure
354 (Table 1, Table S2). Finally, pairwise comparisons of the inbreeding coefficient distributions
355 indicated that the excess of homozygotes was greater in the north than in the south when
356 compared to neutral expectation based on allele frequencies. This was supported with
357 statistically significant differences (non-overlapping confidence intervals and adjusted
358 $P<0.05$) observed in all comparisons except in region pairs 2 and 3; and 4 and 5 (Table 1,
359 Table S2). This indicated that the northern populations are inbreeding more than the
360 southern populations (Table 1, Table S2).

361 A large proportion of SNPs, 25.3%, were polymorphic in all four regions. The fraction of
362 SNPs unique only to one region decreased from going north to south: while 8.6% of the
363 SNPs were unique to region 1, only 2.5% unique SNPs were found in region 4.

364 We did not find support for secondary contact using demographic modelling with
365 Fastsimcoal2. Instead, the null model that included no migration among populations (Figure
366 S6a) received the highest AIC support (Table S3). Parameter priors and estimates, together
367 with their 95% confidence intervals, from the best model are reported in Table S4.

368 DISCUSSION

369 Our results present the first assessment of population structure in the widely distributed bat
370 species, *M. chiloensis*, using individual-based approach with genome-wide markers. We
371 found that geographic distance within the range of the species are reflected in its
372 population structure. Although we found a clear and robust population structure among
373 sampling sites, population structure is correlated with geographical distance, even though
374 populations are separated by ice fields, mountain ranges and stretches of open water. This
375 has implications for the protection of populations that may be susceptible to WNS. Our
376 results also show highest genetic variability in the species is at the southern extent of its
377 range.

378 Strong population structure is rarely seen in bats, even across large geographical scales in
379 genera such as *Myotis*, with shorter dispersal distances (Castella *et al.* 2000; Atterby *et al.*
380 2010; Laine *et al.* 2013). In fact, geographical distance often correlates significantly with

381 genetic distance in bats. This is partially due to autumn migration and swarming behaviour
382 in *Myotis* species, which brings together bats from broad geographic areas to breed and
383 promote recombination (Burns *et al.* 2014; Burns and Broders 2015). Furthermore, powered
384 flight allows effective dispersal, which is often male biased (Arnold 2007; Angell *et al.* 2013).
385 This is reflected in low fixation indices in widespread bat species, such as *M. daubentonii*,
386 where individuals separated by thousands of kilometres in Europe show low fixation indexes
387 (Laine *et al.* 2013). While fixation indices cannot be compared directly across species,
388 especially when different methodological approaches are used, they do give an indication of
389 the connectivity of populations.

390 Although geographic and genetic distances were found to have a strong positive correlation
391 in our study, we can concur that the southernmost population shows a higher degree of
392 isolation compared to the geographic distance to its closest comparative population to the
393 north. An F_{ST} of 0.075 between regions 3 and 4 using whole-genome data is already higher
394 than F_{ST} values recorded for *M. daubentonii* across Europe using microsatellites (Laine *et al.*
395 2013), and in our data, the geographic distance is only c. 1000 km. Our data, with tens of
396 thousands of SNP's also allowed a more precise estimate of fixation compared to a handful
397 of microsatellites. However, due to a limited number of individuals, it did not allow us to
398 examine dispersal as a function of sex, which in bats is often a male driven function (Arnold
399 2007; Laine *et al.* 2013; Angell *et al.* 2013). Our sampling may also have missed some
400 connecting populations in between regions 3 and 4, which could for instance be located on
401 the eastern slopes of the Andes. However, our test for relative contributions of ancestral
402 populations reveals bats in region 4, in the Magallanes and Tierra del Fuego, have no mixing
403 of ancestral populations with the other regions.

404 In the northern hemisphere, approximately 18000 years ago, at the end of the Late
405 Pleistocene, the ice sheets began to recede as the global climate became warmer. The biota
406 migrated northwards following their optimal environments (Huntley and Webb 1989). This
407 expansion of refugial populations has been associated with genetic variation decreasing
408 south-to-north in some species: a trend attributed to a series of bottlenecks when the biota
409 spread from the leading edge of the refugial population, leading to a loss of alleles and
410 decreasing genetic diversity (Hewitt 1996, 1999). Contrary to what one could expect based

411 on these latitudinal shifts in diversity in the northern latitude, genetic diversity in *M.*
412 *chiloensis* appears to increase with increasing latitude, from north to south. We presumed
413 this counterintuitive pattern of heterozygosity within the species may be related to the
414 glaciation history of South America, where populations isolated by glacial events could have
415 been able to hybridize. For instance, in some terrestrial European and Scandinavian
416 vertebrates, the intraspecific genealogical lineages, which formed in separate refugia, were
417 found to have come to secondary contact in the Fennoscandian area (Tegelström 1987;
418 Jaarola and Tegelström 1995; Nesbø *et al.* 1999; Knopp and Merilä 2009).

419 *Myotis chiloensis* is described as a vicariant species with respect to other closely related
420 *Myotis* species (*M. albescens, M. nigricans, M. levis*) from South America, Ruedi et al (2013)
421 estimated this isolation event at 5.5 My in late Miocene. This same time period saw the
422 beginning of a number of glaciations events in Patagonia with variable intensity and
423 duration (Rabassa *et al.* 2011). Glacial episodes isolated the Patagonian forest from around
424 middle Miocene well into the late Quaternary, the Last Glacial Maximum (Rabassa *et al.*
425 2011, Supplemental Figure S7). During the glaciations, the forests on the Pacific coast were
426 most like completely suppressed, possibly with isolated small refugia. On the Atlantic side,
427 the forest was fragmented from 36°S southwards (Sérsic *et al.* 2011). Finally, in Tierra del
428 Fuego the forest was probably displaced towards the current submarine shelf (Ponce *et al.*
429 2011). As the ice retreated refugial populations may have come into secondary contact in
430 the southern part of current range, which could explain the high heterozygosity as well as
431 the small fraction of unique SNP's of these populations. However, our coalescence analysis
432 rejected the secondary contact model, favouring the null model suggesting our study
433 populations are still largely separated after the Last Glacial Maximum. Indeed, the F_{ST} -
434 values are high, suggesting isolation of the populations. By contrast, our analysis for the
435 relative contributions of ancestral populations suggests mixing of populations. One potential
436 explanation for this apparent discrepancy is that we derived Site Frequency Spectrum from
437 a rather small number of individuals, which may carry a signal of migration that is not strong
438 enough to allow a model that includes secondary contact to be favoured over a simpler
439 model without migration.

440 The spread of *P. destructans* via one host to another was very rapid in North America
441 (Blehert *et al.* 2009; Frick *et al.* 2010). This was facilitated in part by the ecology of North
442 American cave-hibernating bats and the availability of suitable environment for the fungus
443 to propagate: limestone caves found throughout the Appalachian region in eastern North
444 America (Lorch *et al.* 2013). Furthermore, as a consequence of down-regulation of
445 metabolism during extended torpor bouts, attempted immune responses fall short, and
446 may even contribute to mortality in hosts infected with *P. destructans* (Field *et al.* 2015;
447 Lilley *et al.* 2017, 2019). In addition to these, the massive population declines associated
448 with WNS in affected species (Turner *et al.* 2011) were magnified by the panmictic
449 population structure across eastern North America in the most affected species, *M.*
450 *lucifugus* (Miller-Butterworth *et al.* 2014; Vonhof *et al.* 2015).

451 Our results for *M. chiloensis* from austral South America suggest the southernmost
452 population in region 4, may be less likely to be infected via their continental conspecifics,
453 because of reduced contact between the populations. Our results indicated no mixing of
454 ancestry in the southernmost individuals in our study, suggesting the *M. chiloensis* on Tierra
455 del Fuego are isolated from their mainland counterparts. To our knowledge, this is also the
456 only population to use extended torpor, a prerequisite for the propagation of *P. destructans*
457 and the onset of WNS (Ossa *et al.* Submitted for publication). Tierra del Fuego, the southern
458 tip of Patagonia and the continent of South America, experiences extended low winter
459 temperatures comparable to areas in North America where WNS is manifested. Our genetic
460 analysis for the presence of *P. destructans* on the sampled bats suggests the fungal
461 pathogen does not exist within the distribution range of our focal species at present. Even if
462 the fungus were to enter the region, variability in host behavior and environmental
463 characteristics may be the primary factors protecting hosts from the pathology related to
464 WNS (Zukal *et al.* 2014, 2016). Most strikingly large cave hibernacula with suitable, stable
465 environmental conditions favouring the environmental persistence of the pathogen in the
466 absence of the hosts, are very scarce and separated by hundreds of kilometers in most of
467 the southern range of *M. chiloensis*.

468 The observed distribution of *M. chiloensis* is vast, covering a range of forested habitats from
469 arid Sclerophyllous to sub-Antartic (Ossa and Rodriguez-San Pedro 2015). In this respect,

470 taking into consideration our results on clear population segregation begs to propose the
471 question on the species status of *M. chiloensis* as a whole. Indeed, *M. chiloensis* also
472 appears to vary phenotypically along its distribution range (Mann 1978; Ossa 2016). It has
473 been proposed that the species was composed of three sub-species: *M. ch. atacamensis*
474 which is presently known as *M. atacamensis; M. ch. arescens* from 29°S to 39°S; and *M. ch.*
475 *chiloensis* from 39°S to 53°S (Mann 1978). That classification was due according to their coat
476 colour changes in relation to exposure to solar radiation and ambient temperature, which is
477 correlated to latitude (Budyko 1969) and levels of precipitation in their habitat. They vary
478 from a lighter pelage to a dark brown colour on a gradient from the northern part of their
479 range to the south (Galaz *et al.* 2006). This promotes the theory, isolation by adaptation, as
480 a driver of population genetic structure. The genetic adaptations of an individual to their
481 local environment separates populations and leads to a reduced gene flow (Orsini *et al.*
482 2013). However, the isolation by adaptation theory negates the fact that there is a
483 possibility of a barrier so that gene flow is inhibited by climate or adaptations to the local
484 environment. It is possible to therefore state that isolation-by-dispersal limitation, and
485 moreover isolation-by- distance, are the more probable causes of the observed results in
486 the present study. Indeed, the reluctance of the species to cross barriers, for instance the
487 Andes, can clearly be seen by examining population 3, where six individuals sampled from
488 Puerto Aysén (437, 442, 443, 167, 256, 260) are visibly isolated on the PCA plot form
489 individuals on the other side of the Andes, under 150 km away. This also depicts the fine
490 scale resolution our individual-based SNP-based approach allows. However, further studies
491 should focus deeper on the taxon status of different population of the species currently
492 recognized as *M. chiloensis*.

493 The results highlight the importance to assess the population structure which may limit the
494 spread of white-nose syndrome disease. Whether *P. destructans* or another epizootic in the
495 future could spread depends largely on the population structure and connectedness of
496 hosts (Lilley *et al.* 2018).

497 ACKNOWLEDGEMENTS

498 We thank the Rufford Foundation (Rufford Small Grant 10502-1 and 23042-2), H2020 Marie
499 Skłodowska-Curie Actions (706196), and Ohio University Research Council for funding the

work. We thank Servicio Agricola y ganadero Diproren for the capture permits in Tierra del Fuego (Res Ex: 1253/2016 and 4924/2017), Juan Carlos Aravena from the Instituto de la Patagonia for his help, the personnel from WCS Chile for allowing us to conduct research at Karukinka Natural Reserve as well as for their help with field work. We thank Michelle Lineros and Tania Gatica from the National Health Institute for their help to obtain the tissue samples. We thank Austin Waag for assistance with field work.

REFERENCES

Angell, R. L., R. K. Butlin, and J. D. Altringham, 2013 Sexual segregation and flexible mating patterns in temperate bats. Plos One 8:.

Arnold, B. D., 2007 Population structure and sex-biased dispersal in the forest dwelling vespertilionid bat, *Myotis septentrionalis*. Am. Midl. Nat. 157: 374–384.

Atterby, H., J. Aegerter, G. Smith, C. Conyers, T. Allnutt *et al.*, 2010 Population genetic structure of the Daubenton's bat (*Myotis daubentonii*) in western Europe and the associated occurrence of rabies. Eur. J. Wildl. Res. 56: 67–81.

Blehert, D. S., A. C. Hicks, M. Behr, C. U. Meteyer, B. M. Berlowski-Zier *et al.*, 2009 Bat white-nose syndrome: an emerging fungal pathogen? Science 323: 227–227.

Bohonak, A. J., 1999 Dispersal, gene flow, and population structure. Q. Rev. Biol. 74: 21–45.

Bozinovic, F., L. Contreras, M. Rosenmann, and J. Torres-Mura, 1985 Bioenergetics of *Myotis chiloensis* (Quiroptera: Vespertilionidae). Rev Chil Hist Nat 58: 39–45.

Budyko, M. I., 1969 The effect of solar radiation variations on the climate of the Earth. Tellus 21: 611–619.

521 Burland, T. M., and J. W. Wilmer, 2001 Seeing in the dark: molecular approaches to the
522 study of bat populations. Biol. Rev. 76: 389–409.

523 Burns, L. E., and H. G. Broders, 2015 Who swarms with whom? Group dynamics of *Myotis*
524 bats during autumn swarming. Behav. Ecol. 26: 866–876.

525 Burns, L. E., T. R. Frasier, and H. G. Broders, 2014 Genetic connectivity among swarming
526 sites in the wide ranging and recently declining little brown bat (*Myotis lucifugus*).
527 Ecol. Evol. 4: 4130–4149.

528 Campbell, L. J., D. P. Walsh, D. S. Blehert, and J. M. Lorch, 2019 Long-term survival of
529 *Pseudogymnoascus destructans* at elevated temperatures. J. Wildl. Dis.

530 Cangelosi, G., N. Freitag, and M. Riley-Buckley, 2004 From outside to inside: environmental
531 microorganisms as human pathogens. *American Society of Microbiology*.

532 Castella, V., M. Ruedi, L. Excoffier, C. Ibanez, R. Arlettaz *et al.*, 2000 Is the Gibraltar Strait a
533 barrier to gene flow for the bat *Myotis myotis* (Chiroptera: Vespertilionidae)? Mol.
534 Ecol. 9: 1761–1772.

535 Cockrum, E., 1969 Migration in the guano bat, *Tadarida brasiliensis*. Misc Publ Mus Nat Hist
536 Univ Kans. 51: 303–336.

537 Elshire, R. J., J. C. Glaubitz, Q. Sun, J. A. Poland, K. Kawamoto *et al.*, 2011 A robust, simple
538 genotyping-by-sequencing (GBS) approach for high diversity species (L. Orban, Ed.).
539 PLoS ONE 6: e19379.

540 Escobar, L. E., A. Lira-Noriega, G. Medina-Vogel, and A. T. Peterson, 2014 Potential for
541 spread of the white-nose fungus (*Pseudogymnoascus destructans*) in the Americas:

use of Maxent and NicheA to assure strict model transference. Geospatial Health 221–229.

Excoffier, L., I. Dupanloup, E. Huerta-Sánchez, V. C. Sousa, and M. Foll, 2013 Robust Demographic Inference from Genomic and SNP Data. PLOS Genet. 9: e1003905.

Field, K. A., J. Johnson, T. Lilley, S. Reeder, E. Rogers *et al.*, 2015 The white-nose syndrome transcriptome: activation of anti-fungal host responses in wing tissue of hibernating bats. Plos Pathog. 11: e1005168.

Frick, W. F., J. F. Pollock, A. C. Hicks, K. E. Langwig, D. S. Reynolds *et al.*, 2010 An emerging disease causes regional population collapse of a common North American bat species. Science 329: 679–682.

Galaz, J., J. Yañez, A. Gantz, and D. Martínez, 2006 Orden Chiroptera. Pp. 67–89 in Mamíferos de Chile (A. Muñoz-Pedreros and J.Yañez, eds.)., in *Mamíferos de Chile*, Centro de Estudios Agrarios y Ambientales, Valdivia, Chile.

Gardner, A. (ed.), 2007 *Mammals of South America, Volume 1*. University of Chicago Press, Chicago, Illinois.

Glass, B. P., 1982 Seasonal movements of Mexican freetail bats *Tadarida brasiliensis mexicana* banded in the Great Plains. Southwest. Nat. 27: 127–133.

Hewitt, G. M., 1999 Post-glacial re-colonization of European biota. Biol. J. Linn. Soc. 68: 87–112.

Hewitt, G. M., 1996 Some genetic consequences of ice ages, and their role in divergence and speciation. Biol. J. Linn. Soc. 58: 247–276.

563 Holz, P., J. Hufschmid, W. Boardman, P. Cassey, S. Firestone *et al.*, 2019 Does the fungus
564 causing white-nose syndrome pose a significant risk to Australian bats? Wildl. Res.
565 46: 657–668.

566 Hoyt, J. R., K. E. Langwig, J. Okoniewski, W. F. Frick, W. B. Stone *et al.*, 2014 Long-term
567 persistence of *Pseudogymnoascus destructans*, the causative agent of white-nose
568 syndrome, in the absence of bats. EcoHealth.

569 Huntley, B., and T. Webb, 1989 Migration: species' response to climatic variations caused by
570 changes in the earth's orbit. J. Biogeogr. 5–19.

571 Jaarola, M., and H. Tegelström, 1995 Colonization history of north European field voles
572 (*Microtus agrestis*) revealed by mitochondrial DNA. Mol. Ecol. 4: 299–310.

573 Johnson, J. S., D. M. Reeder, T. M. Lilley, G. Á. Czirják, C. C. Voigt *et al.*, 2015 Antibodies to
574 *Pseudogymnoascus destructans* are not sufficient for protection against white-nose
575 syndrome. Ecol. Evol. 2203–2214.

576 Knopp, T., and J. Merilä, 2009 The postglacial recolonization of Northern Europe by *Rana*
577 *arvalis* as revealed by microsatellite and mitochondrial DNA analyses. Heredity 102:
578 174–181.

579 Koopman, K., 1967 The southernmost bats. J. Mammal. 48: 487–488.

580 Laine, V. N., T. M. Lilley, K. Norrdahl, and C. R. Primmer, 2013 Population genetics of
581 Daubenton's bat (*Myotis daubentonii*) in the Archipelago Sea, SW Finland. Ann. Zool.
582 Fenn. 50: 303–315.

583 Lemopoulos, A., S. Uusi-Heikkilä, A. Vasemägi, A. Huusko, H. Kokko *et al.*, 2017 Genome-
584 wide divergence patterns support fine-scaled genetic structuring associated with
585 migration tendency in brown trout. Can. J. Fish. Aquat. Sci. 75: 1680–1692.

586 Leopardi, S., D. Blake, and S. J. Puechmaille, 2015 White-nose syndrome fungus introduced
587 from Europe to North America. Curr. Biol. 25: R217–R219.

588 Lilley, T., J. Anttila, and L. Ruokolainen, 2018 Landscape structure and ecology influence the
589 spread of a bat fungal disease. Funct. Ecol. 32: 2483–2496.

590 Lilley, T. M., J. M. Prokkola, A. S. Blomberg, S. Paterson, J. S. Johnson *et al.*, 2019 Resistance
591 is futile: RNA-sequencing reveals differing responses to bat fungal pathogen in
592 Nearctic *Myotis lucifugus* and Palearctic *Myotis myotis*. Oecologia.

593 Lilley, T. M., J. M. Prokkola, J. S. Johnson, E. J. Rogers, S. Gronsky *et al.*, 2017 Immune
594 responses in hibernating little brown myotis (*Myotis lucifugus*) with white-nose
595 syndrome. Proc R Soc B 284: 20162232.

596 Lorch, J. M., C. U. Meteyer, M. J. Behr, J. G. Boyles, P. M. Cryan *et al.*, 2011 Experimental
597 infection of bats with *Geomyces destructans* causes white-nose syndrome. Nature
598 480: 376-U129.

599 Lorch, J. M., L. K. Muller, R. E. Russell, M. O'Connor, D. L. Lindner *et al.*, 2013 Distribution
600 and environmental persistence of the causative agent of white-nose syndrome,
601 *Geomyces destructans*, in bat hibernacula of the Eastern United States. Appl.
602 Environ. Microbiol. 79: 1293–1301.

603 Mann, G., 1978 Los pequeños mamiferos de Chile. Gayana Concepc. 40: 1–342.

604 Mansilla, C. A., R. D. McCulloch, and F. Morello, 2018 The vulnerability of the Nothofagus
605 forest-steppe ecotone to climate change: Palaeoecological evidence from Tierra del
606 Fuego (~53°S). Palaeogeogr. Palaeoclimatol. Palaeoecol. 508: 59–70.

607 McCracken, G. F., R. F. Bernard, M. Gamba-Rios, R. Wolfe, J. J. Krauel *et al.*, 2018 Rapid
608 range expansion of the Brazilian free-tailed bat in the southeastern United States,
609 2008–2016. J. Mammal. 99: 312–320.

610 Meierhofer, M. B., J. S. Johnson, S. J. Leivers, B. L. Pierce, J. E. Evans *et al.*, 2019 Winter
611 habitats of bats in Texas. PLOS ONE 14: e0220839.

612 Miller-Butterworth, C. M., M. J. Vonhof, J. Rosenstern, G. G. Turner, and A. L. Russell, 2014
613 Genetic structure of little brown bats (*Myotis lucifugus*) corresponds with spread of
614 white-nose syndrome among hibernacula. J. Hered. esu012.

615 Moritz, C., 1994 Defining 'Evolutionarily Significant Units' for conservation. Trends Ecol.
616 Evol. 9: 373–375.

617 Muller, L. K., J. M. Lorch, D. L. Lindner, M. O'Connor, A. Gargas *et al.*, 2013 Bat white-nose
618 syndrome: a real-time TaqMan polymerase chain reaction test targeting the
619 intergenic spacer region of *Geomyces destructans*. Mycologia 105: 253–259.

620 Nesbø, C. L., T. Fossheim, L. A. Vøllestad, and K. S. Jakobsen, 1999 Genetic divergence and
621 phylogeographic relationships among European perch (*Perca fluviatilis*) populations
622 reflect glacial refugia and postglacial colonization. Mol. Ecol. 8: 1387–1404.

623 Ommundsen, P., C. Lausen, and L. Matthias, 2017 First acoustic records of the Brazilian free-
624 tailed bat (*Tadarida brasiliensis*) in British Columbia. Northwest. Nat. 98: 132–136.

625 Orsini, L., J. Vanoverbeke, I. Swillen, J. Mergeay, and L. De Meester, 2013 Drivers of
626 population genetic differentiation in the wild: isolation by dispersal limitation,
627 isolation by adaptation and isolation by colonization. Mol. Ecol. 22: 5983–5999.

628 Ossa, G., 2016 Primer registro de la especie *Myotis chiloensis*, (Waterhouse, 1838)
629 (Chiroptera, Vespertilionidae) en el Parque Nacional Alberto de Agostini (Región de
630 Magallanes y Antártica Chilena). An. Inst. Patagon. 44: 85–88.

631 Ossa, G., J. S. Johnson, A. I. E. Puisto, V. Rinne, I. E. Sääksjärvi *et al.*, 2019 The Klingon
632 batbugs: Morphological adaptations in the primitive bat bugs, *Bucimex chilensis* and
633 *Primicimex cavernis*, including updated phylogeny of Cimicidae. Ecol. Evol. 9: 1736–
634 1749.

635 Ossa, G., T. M. Lilley, A. G. Waag, M. Meierhofer, and J. Johnson, Submitted for publication
636 Roosting ecology of the southernmost tree-dwelling bats, *Myotis chiloensis* and
637 *Histiotus magellanicus*, in southern Tierra del Fuego.

638 Ossa, G., and Rodriguez-San Pedro, 2015 *Myotis chiloensis* (Chiroptera: Vespertilionidae).
639 Mammal Species 47: 51–56.

640 Ponce, J. F., J. Rabassa, A. Coronato, and A. M. Borromei, 2011 Palaeogeographical evolution
641 of the Atlantic coast of Pampa and Patagonia from the last glacial maximum to the
642 Middle Holocene. Biol. J. Linn. Soc. 103: 363–379.

643 Rabassa, J., A. Coronato, and O. Martínez, 2011 Late Cenozoic glaciations in Patagonia and
644 Tierra del Fuego: an updated review. Biol. J. Linn. Soc. 103: 316–335.

645 Raudabaugh, D. B., and A. N. Miller, 2013 Nutritional capability of and substrate suitability
646 for *Pseudogymnoascus destructans*, the causal agent of wat white-nose syndrome.
647 PLoS ONE 8: e78300.

648 Ruedi, M., B. Stadelmann, Y. Gager, E. J. P. Douzery, C. M. Francis *et al.*, 2013 Molecular
649 phylogenetic reconstructions identify East Asia as the cradle for the evolution of the
650 cosmopolitan genus Myotis (Mammalia, Chiroptera). Mol. Phylogenet. Evol. 69: 437–
651 449.

652 Scholthof, K.-B. G., 2007 The disease triangle: pathogens, the environment and society. Nat.
653 Rev. Microbiol. 5: 152–156.

654 Semenza, J. C., and B. Menne, 2009 Climate change and infectious diseases in Europe.
655 Lancet Infect. Dis. 9: 365–375.

656 Serre, J., 2006 *Génétique des populations*. Dunod, Paris.

657 Sérsic, A. N., A. Cosacov, A. A. Cocucci, L. A. Johnson, R. Pozner *et al.*, 2011 Emerging
658 phylogeographical patterns of plants and terrestrial vertebrates from Patagonia.
659 Biol. J. Linn. Soc. 103: 475–494.

660 Tegelström, H., 1987 Transfer of mitochondrial DNA from the northern red-backed vole
661 (*Clethrionomys rutilus*) to the bank vole (*C. glareolus*). J. Mol. Evol. 24: 218–227.

662 Turbill, C., and J. A. Welbergen, 2019 Anticipating white-nose syndrome in the Southern
663 Hemisphere: Widespread conditions favourable to *Pseudogymnoascus destructans*
664 pose a serious risk to Australia's bat fauna. Austral Ecol. 45: 89–96.

665 Turner, G. G., D. M. Reeder, and J. T. H. Coleman, 2011 A five-year assessment of mortality
666 and geographic spread of white-nose syndrome in North American bats and a look to
667 the future. Bat Res. News 52: 13–27.

668 Verant, M. L., J. G. Boyles, W. Waldrep, G. Wibbelt, and D. S. Blehert, 2012 Temperature-
669 dependent growth of *Geomyces destructans*, the fungus that causes bat white-nose
670 syndrome. Plos One 7: e46280.

671 Vonhof, M. J., A. L. Russell, and C. M. Miller-Butterworth, 2015 Range-wide genetic analysis
672 of little brown bat (*Myotis lucifugus*) populations: estimating the risk of spread of
673 White-nose syndrome. PLoS ONE 10: e0128713.

674 Warnecke, L., J. M. Turner, T. K. Bollinger, J. M. Lorch, V. Misra *et al.*, 2012 Inoculation of
675 bats with European *Geomyces destructans* supports the novel pathogen hypothesis
676 for the origin of white-nose syndrome. Proc. Natl. Acad. Sci. U. S. A. 109: 6999–7003.

677 Wilder, A. P., T. H. Kunz, and M. D. Sorenson, 2015 Population genetic structure of a
678 common host predicts the spread of white-nose syndrome, an emerging infectious
679 disease in bats. Mol. Ecol. 24: 5495–5506.

680 Zukal, J., H. Bandouchova, T. Bartonicka, H. Berkova, V. Brack *et al.*, 2014 White-nose
681 syndrome fungus: a generalist pathogen of hibernating bats. Plos One 9: e97224.

682 Zukal, J., H. Bandouchova, J. Brichta, A. Cmokova, K. S. Jaron *et al.*, 2016 White-nose
683 syndrome without borders: *Pseudogymnoascus destructans* infection tolerated in
684 Europe and Palearctic Asia but not in North America. Sci. Rep. 6: 19829.

685

686 Figure captions:

687 Figure 1. Sampling locations and groupings for genetic sampling of *Myotis chiloensis* in Chile
688 (A). The two most important principal components calculated from allele frequencies
689 explain 15.8% of the total nucleotide variation (B).

690 Figure 2. Biogeographical ancestry (admixture) analysis based on nucleotide polymorphisms.
691 Each vertical bar represents an individual, ordered by latitude. Red, green, blue and purple
692 colours indicate the relative genetic contributions of ancestral populations inhabiting
693 regions 1-4, respectively.

694 Fig. 3. The correlation between geographic and genetic distances between individuals.
695 Geographic distances are measured in kilometres, and genetic distances as Euclidean
696 principal component distances from the reference individual (sample 700). Dashed lines
697 represent 95% confidence interval for the linear model. The violin plot highlights the
698 differences between model residuals for each study region. Residual distributions that differ
699 significantly from zero after Bonferroni correction for multiple testing are marked with * (P
700 < 0.05) and *** ($P < 0.0001$).

701

Numeric region	Number of individuals (A)	Number of duplicates (B)	male / female	Mean observed heterozygosity (95% confidence interval)	Mean expected heterozygosity (95% confidence interval)	Inbreeding coefficient *F*	Unique SNPs
1	20	6	16/4	0.2550 (0.2530-0.2570)	0.2793 (0.2777-0.2809)	0.0868 (0.0813 - 0.0925)	8.6%
2	19	6	9/10	0.2536 (0.2514-0.2557)	0.2765 (0.2749-0.2780)	0.08286 (0.0773- 0.0891)	4.4%
3	14	9	7/7	0.2872 (0.2848-0.2896)	0.2993 (0.29762-0.3009)	0.0404 (0.0343 – 0.0463)	3.6%
4	13	9	5/8	0.3248 (0.3221-0.3275)	0.3335 (0.3316-0.3352)	0.0261 (0.0197 – 0.0326)	2.5%
tot.	**66**	**30**					

Table 1. Individuals and samples per region.

	F_{ST} and mean geographic distance (*km*)			
	Region 4	Region 3	Region 2	Region 1
Region 4		*970.9*	*1550.3*	*2266.9*
Region 3	0.075***		*588.7*	*1326.6*
Region 2	0.089***	0.041***		*757.0*
Region 1	0.113***	0.072***	0.040***	

Table 2. Nei's pairwise F_{ST} and geographic distances (in italics) between populations inhabiting the four geographic regions. The significance level (P<0.01) of the F_{ST} statistics is denoted with ***.

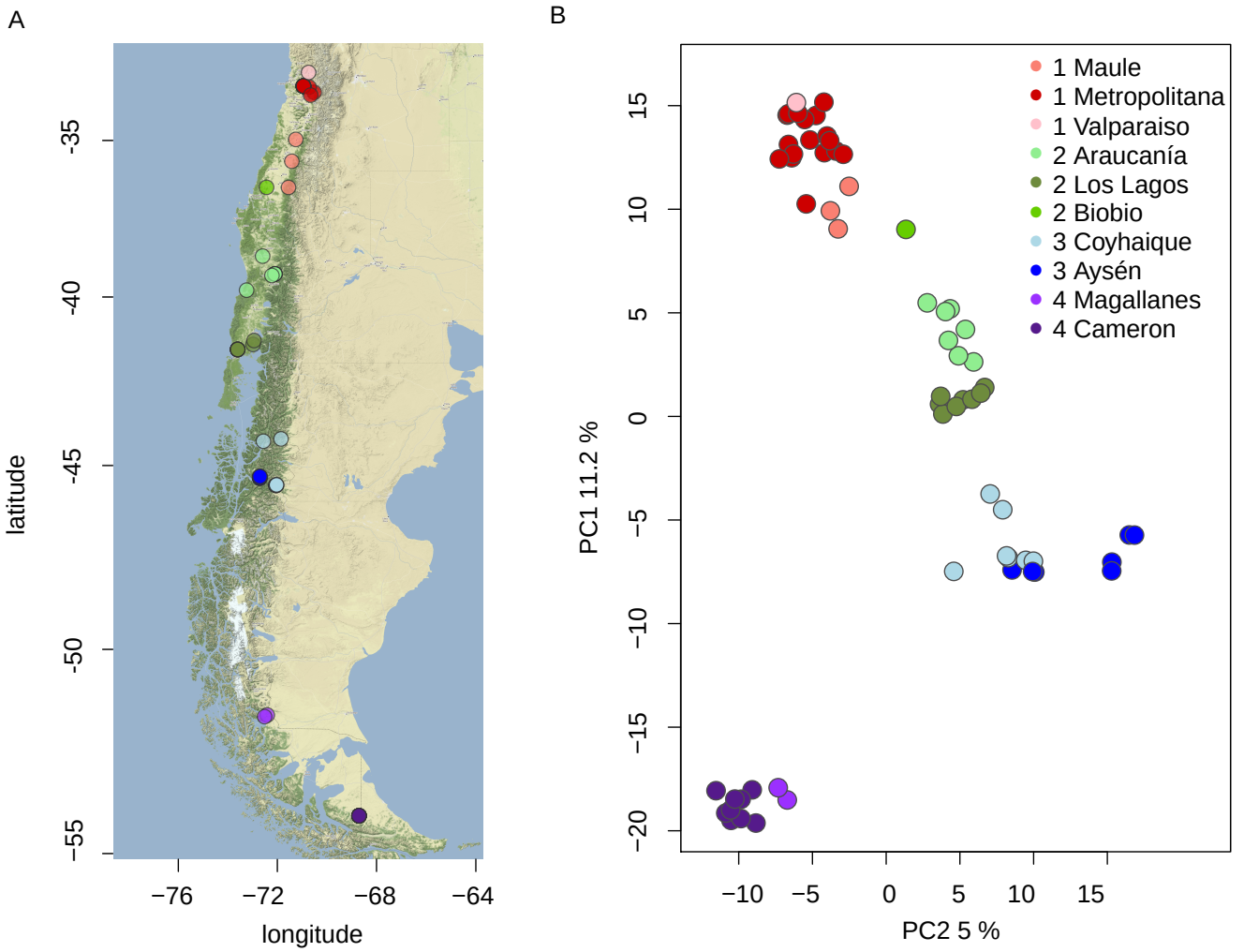
A
B
latitude
longitude
-35
-40
-45
-50
−55
−76
−72
−68
−64
PC1 11.2 %
PC2 5 %
15
10
5
0
−5
−10
−15
−20
−10
−5
0
5
10
15
1 Maule
1 Metropolitana
1 Valparaiso
2 Araucanía
2 Los Lagos
2 Biobio
3 Coyhaique
3 Aysén
4 Magallanes
4 Cameron

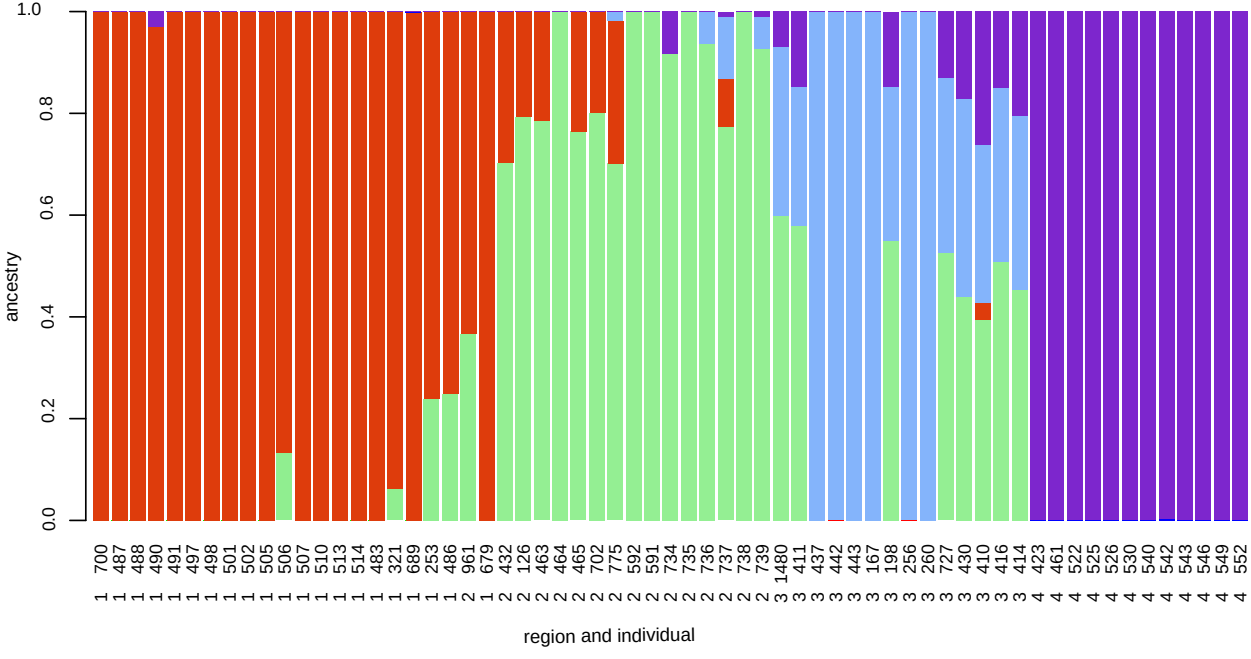
ancestry
0.0
0.2
0.4
0.6
0.8
1.0
1 700
1 487
1 488
1 490
1 491
1 497
1 498
1 501
1 502
1 505
1 506
1 507
1 510
1 513
1 514
1 483
1 321
1 689
1 253
1 486
2 961
1 679
2 432
2 126
2 463
2 464
2 465
2 702
2 775
2 592
2 591
2 734
2 735
2 736
2 737
2 738
2 739
3 1480
3 411
3 437
3 442
3 443
3 167
3 198
3 256
3 260
3 727
3 430
3 410
3 416
3 414
4 423
4 461
4 522
4 525
4 526
4 530
4 540
4 542
4 543
4 546
4 549
4 552
region and individual

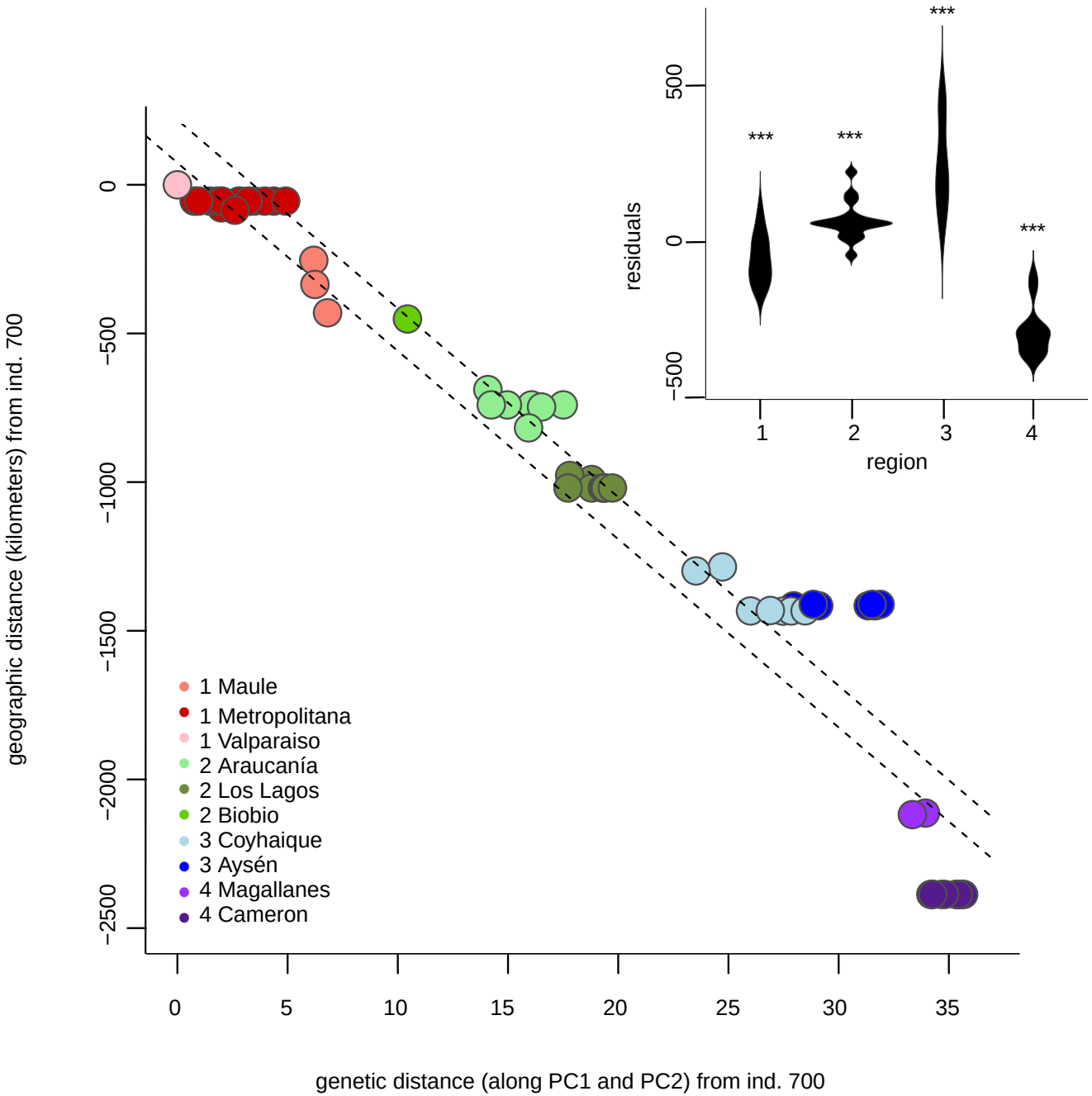
geographic distance (kilometers) from ind. 700
genetic distance (along PC1 and PC2) from ind. 700
0
−500
−1000
−1500
−2000
−2500
0
5
10
15
20
25
30
35
1 Maule
1 Metropolitana
1 Valparaiso
2 Araucanía
2 Los Lagos
2 Biobio
3 Coyhaique
3 Aysén
4 Magallanes
4 Cameron
residuals
500
0
−500
***
***
***
***
1
2
3
4
region